*Structural Eng. / Earthquake Eng. Vol. 3. No. 2, 287s-295s. October 1986*
*Japan Society of Civil Engineers (Proc. of JSCE No. 374 / I-6)*

# STRENGTH CHARACTERISTICS OF STEEL ARCH BRIDGES SUBJECTED TO LONGITUDINAL ACCELERATION

*By Shigeru KURANISHI* and Akinori NAKAJIMA***

The fundamental in-plane dynamic characteristics as well as the failure of two-hinged arch ribs subjected to the harmonic excitation and earthquake ground motion are investigated in this paper. In the analyses, the yielding of materials is taken into account in the finite deformations. Furthermore, the dynamic characteristics of stiffened deck arch bridges are presented paying special attention to the influence of the stiffening girder, its connection to the arch rib and the supporting conditions on the resisting capacity of arch bridges against the harmonic excitation.

*Keywords* : *arch bridge, elasto-plastic vibration, aseismic design*

## 1. INTRODUCTION

A number of studies have been carried out on the ultimate strength characteristics of arch structures under the static loads to establish a rational design method based on the concept of limit state[1),2)] and some proposals are made for the practical design code[3),4)].

However, very few studies take into account the real structural configurations of arch bridges and the dynamic effects of the excitations, for example, by the earthquake and the fluctuating wind action. Furthermore, the researchers' interest has been limited within the elastic problems of the dynamic instability of arches, and thus the structural failure caused by the combined action of yielding of materials and the instability has not always been considered.

For example, Aida et al[5)]. determined the region of the dynamic instability of arches under the various periodic loads. Gregory and Plaut[6)] investigated the dynamic snap-through-type instability of shallow arches under impulsive loadings, and determined the critical load numerically. However, only the elastic arches were considered in these works.

The fundamental mode of vibration of arches is antisymmetric with one node at the crown which moves longitudinally. This mode is similar to that of the one-story rigid frames and is susceptible to the longitudinal motion of supports caused by such as the earthquake ground motion. Moreover, since the deck type of the actual arch bridges generally have deck girders or stiffening girders to carry the floor system, it becomes much more complicated to make their dynamic models. The mass, stiffness, connecting details of the arch ribs at the crown and supporting conditions of the girder will all affect the dynamic characteristics and will change the resisting capacity against the earthquake.

* Member of JSCE, Dr. of Engrg., Professor, Dept. of Civil Engrg., Tohoku Univ. (Sendai 980 Japan)
** Member of JSCE, Dr. of Engrg., Research Associate, Dept. of Civil Engrg., Utsunomiya Univ. (Utsunomiya 321 Japan)

For example, the present design method recommends the stiffening girder to be connected rigidly to the crown. In such arches, the longitudinal component of the inertia force of the girder due to the earthquake ground motion will becomes larger depending on the degree of rigidity of the connection at the crown, where a short column is occasionally installed. Then this short column will suffer the stress concentration during earthquakes, and the inertia force of the girder that transmit to the support through the arch rib may have unfavorable effects. At present, there is no definite answer to how much stiffness is required in this short column.

The alternative way of designing is to fix the end support of the girder against the longitudinal movement so that the arch bridge can resist the earthquake through the girders. This fixed support can also prevent the longitudinal motion of the arch rib and suppress the antisymmetrical vibrational mode. Therefore, the dynamic characteristics of arch bridges may change significantly depening on the supporting conditions of the stiffening girder. Consequently, more reasonable seismic design is expected after the true strength and behavior of such actual structures are studied properly and extensively in view of the concept of the limit state design.

In this paper, the fundamental in-plane dynamic characteristics as well as the failure of the two-hinged steel arch ribs subjected to the harmonic excitation and earthquake ground motion are studied. In the analyses, the yielding of materials is taken into account in finite deformations. Special attention is paid to the influence of the stiffening girder, its connection to the arch rib and the supporting conditions upon the resisting capacity of deck type of arch bridges against the harmonic excitations.

## 2. NUMERICAL MODELS AND PARAMETERS

An incremental method with the modified Newton-Raphson iteration scheme is employed to solve the finite deformation problems which include the geometrical nonlinearity and yielding of materials. Newmark's $\beta$ method ($\beta=1/4$) is used to evaluate the dynamic responses of structures. These numerical methods have been explained in Ref. (7).

Fig. 1 shows the configurations of parabolic two-hinged steel arch ribs and arch bridge structures with the stiffening deck to be analyzed here. The span length of arch ribs $L$ is 100 m and the rise $f$ is 15 m. The slenderness ratio of an arch rib $\lambda_A$ is defined in terms of the arc length along the arch axis $L_S$ and the radius of gyration of a cross section. The stiffness ratio $\tau$ is defined as the ratio of the cross-sectional moment of inertia of an arch rib to that of a stiffening girder. The slenderness ratio $\lambda_A$ is choosen to be 150, 200, or 300, and the ratio $\tau$ is set 0.5, 1.0 and 2.0 considering the current actual arch bridge designing. The ratio $\tau$ which is equal to 1 000 is also employed to estimate the behavior of the deck type of the two-hinged arch bridge. The influence of the following three types of longitudinal supporting conditions of the stiffening girder on the resisting capacity of the arch bridges is examined here : (1) both ends are movable hinges; (2) both ends are supported by fixed hinges; (3) one end is supported by a roller and the other by a fixed hinge. Moreover two types of the structural details at the crown are compared. One type has the rigid connection between the stiffening girder and the arch rib, and another detail has a central post between the arch rib and the stiffening girder as shown in Fig. 1.

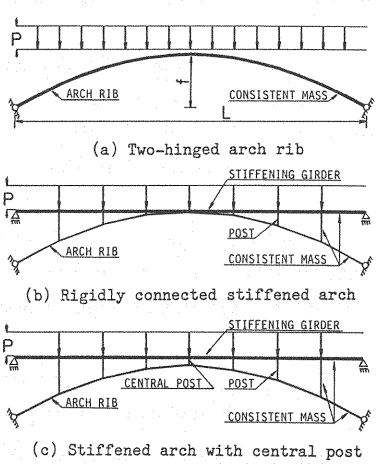


Fig. 1 Configurations of arch structures.

The arch ribs and posts have boxed cross sections and the stiffening girders have I-cross sections. The cross-sectional moment of inertia of the central post is arranged ten times of that of the other posts. Fig. 2 indicates the proportions of cross sections of an arch rib, stiffening girder and post. In the finite

element analyses, 16 elements are used to analyze the two-hinged arch ribs, and as for arch bridges with the stiffening girder, both the arch rib and the stiffening girder are divided into 8 elements, but the post is treated as one element and rigidly connected to the arch rib and the stiffening girder.

In these analyses, mass of slabs is add to mass of arch ribs or stiffening girders and its effect is then examined by artificially varying the mass density of arch ribs or stiffening girders. The effect of axial forces on the ultimate strength of arch structures is examined by applying the static vertical forces on the arch ribs for two-hinged arch ribs but by applying the forces on the arch ribs through the stiffening girders for stiffened deck arch bridges. The loading patterns are also given in Fig. 1. Unless otherwise specified, each nodal load $P$ is taken as a half of the static ultimate nodal load $P_{max}$ in this loading patterns. In practice, it is usually considered that the dead load intensity becomes about 80 % of the design load, which becomes approximately equal to the static ultimate load divided by safety factor (=1.7). The excitations applied at the support are the longitudinal sinusoidal acceleration whose period is equal to the first natural period of the arch structure and the N-S component of the acceleration of the 1940 El-Centro earthquake. In this paper, the ideal elasto-plastic stress-strain relationship is assumed for steel, and the residual stress is not considered. Young's modulus is 206 GN/m$^2$, and the yield stress is 235 MN/m$^2$. The effect of the hysteretic damping is considered to be much more significant than that of the structural damping in the cases taken up here, so the structural damping is ignored. The presentation of the structural damping brings out generally more conservative results than those without the structural damping.

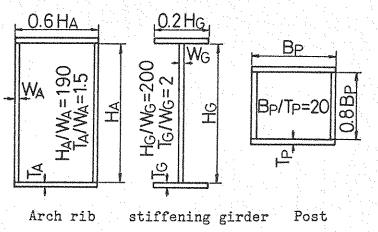


Fig. 2 Proportions of cross section.

## 3. DYNAMIC STRENGTH CHARACTERISTICS OF TWO-HINGED ARCH RIB

### (1) Dynamic strength characteristics under harmonic excitation

When two-hinged arch ribs are subjected to the sinusoidal acceleration whose period is equal to the first natural period of the arch structure, the first antisymmetrical vibrational mode appears and its amplitude develops rapidly to initiate yielding in a cross section. A typical result of vertical displacement responses at 1/4, 1/2 and 3/4 points of an arch span is shown in Fig. 3, in which the slenderness ratio of the arch rib $\lambda_A$ is 200 and the amplitude of the sinusoidal acceleration $Z$ is 0.3 m/s$^2$. The ordinate shows the vertical displacement normalized by the arch span, and the abscissa is the elapse time normalized by the first natural period. A circle in this figure indicates the inception point of yielding in the cross section. By the combined action of the hysteretic nature of yielding and $P$-$\Delta$ effect of compressive axial force, the displacement begins to shift gradually to one direction. Finally the displacement diverges and the arch will collapse. These dynamic behavior is essentially the same as that of columns subjected to the sinusoidal acceleration discussed in Ref. (7). The yielded zones of arch rib (shaded portions) at the ultimate state are also shown in Fig. 3. It is noted that the plastic hinges are finally formed at 1/4 and 3/4 points of the arch rib after the yielded zones spread extensively. The process up to collapse is common to all kinds of arch ribs analyzed here and is independent of their slenderness ratios.

It is shown in Fig. 4. whether the two-hinged arch ribs collapse or not within ten cycles of application of the sinusoidal acceleration. (The application of ten cycles of the sinusoidal excitation is considered to be usually enough to judge the ultimate state of structures referring to the study previously done by authors[7]. Therefore, the dynamic strength of arch structures is defined by its collapse within ten-cycle loading hereafter.) While the triangles indicate that the two-hinged arch rib collapses within ten cycles of application of the sinusoidal acceleration, the circles indicate that the arch rib does not collapse. The ordinate presents the amplitude of the sinusoidal acceleration, and the slenderness ratio is given in its abscissa. Two-hinged arch ribs have a tendency to lose their dynamic strength as the slenderness ratio

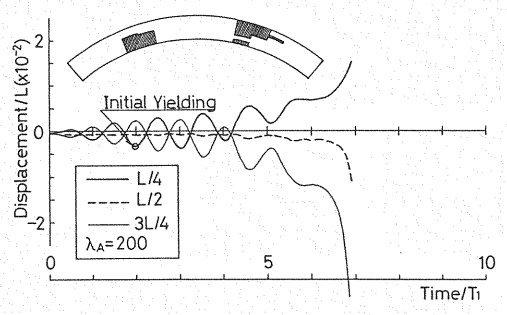


Fig. 3 Vertical displacement response of arch rib under sinusoidal acceleration.

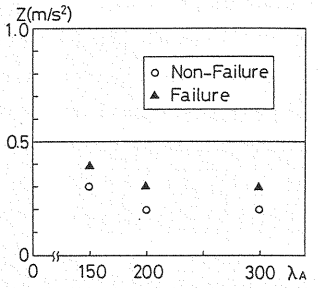


Fig. 4 Relationship between slenderness ratio and dynamic strength.

becomes larger, although there exists only a slight difference in the dynamic strength.

(2) Dynamic strength characteristics under 1940 El-Centro earthquake

The initial eight seconds of N-S component of the acceleration record of the 1940 El-Centro earthquake as shown in Fig. 5 whose peak acceleration is 3.45 m/s² is used as a input ground motion. The two-hinged arch rib vibrates in the first antisymmetrical mode excited by this earthquake. However, the vibrational amplitude grows up to small extent and the maximum fiber stress becomes about 80 % of the yield point. When earthquakes to be applied are larger than the El-Centro earthquake, cross sections of the arch rib will probably yield and the arch structure may collapse. Fig. 6 shows the vertical displacement responses of 1/4, 1/2 and 3/4 points of the arch rib to the earthquake of three times of the El-Centro earthquake for the two-hinged arch rib whose slenderness ratio $\lambda_A$=200. After about 2.5 seconds, the initial yielding occurs in a cross section. In spite of diminishing acceleration amplitude of the El-Centro N-S component after about 6 seconds, the displacement increases gradually and the two-hinged arch rib is considered to be in the collapse state. The process up to collapse by the El-Centro earthquake is almost the same as that by the sinusoidal acceleration.

If the gravity mass load becomes heavier than a half of the static ultimate load and the effect of the axial force by the load becomes more severe, the arch rib may collapse by the original El-Centro earthquake. When the two-hinged arch rib is subjected to the gravity mass load which is 0.8 times of the static ultimate load, a cross section yields but the arch rib does not collapse. Fig. 7 shows the vertical displacement response of the arch rib under the static force corresponding to the gravity mass load of 0.9 times of the static ultimate load. By the applied large compressive axial force, cross sections yield in spite of the small

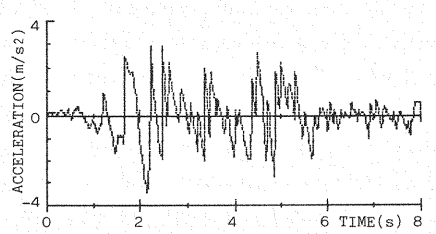


Fig. 5 1940 El-Centro N-S component.

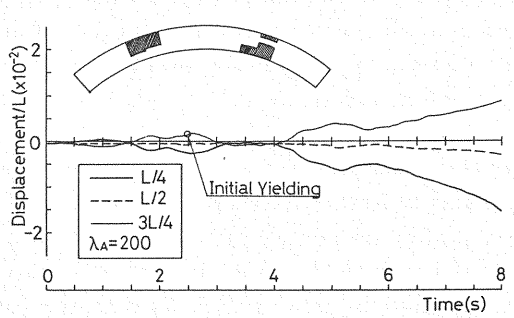


Fig. 6 Vertical displacement response of arch rib under three times of 1940 El-Centro N-S component.

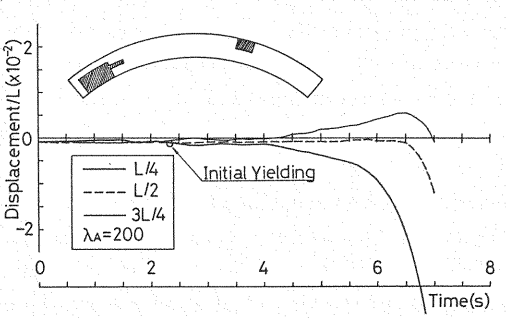


Fig. 7 Vertical displacement response of arch rib under 1940 El-Centro N-S component.

vibrational amplitude. The antisymmetrical displacement increase rapidly and the two-hinged arch rib collapses. This implies that the static ultimate strength of the two-hinged arch rib shows a decrease of about 10 % by the dynamic effect of the El-Centro earthquake.

## 4. DYNAMIC STRENGTH CHARACTERISTICS OF TWO-HINGED ARCH BRIDGE WITH STIFFENING DECK

### (1) Influence of flexural rigidity ratio of arch rib to stiffening girder

In the next step, the dynamic strength characteristics of two-hinged arch bridges with a stiffening girder is investigated in consideration of the actual arch bridge configurations, where the slenderness ratio of the arch rib $\lambda_A$ is fixed to be 200 and the ratio of the flexural rigidity of the arch rib to that of the stiffening girder $\tau$ is varied. Fig. 8 shows the vertical displacement responses of 1/4, 1/2 and 3/4 points of the arch rib for $\tau=1.0$ and $Z=2.0\ \mathrm{m/s^2}$. The process up to collapse of the arch bridge with the stiffening deck is the same as the case of the two-hinged arch rib, where the antisymmetrical displacement also increases rapidly. The yielded zones of cross sections in the ultimate state is also illustrated in Fig. 8. The yielded zones spread remarkably in the stiffening girder's and the posts' cross sections, and two plastic hinges are also finally formed in the arch rib's cross sections. The ratio $\tau$ does not affect on the spreading manner of the yielded zones into the cross sections except for the posts' cross sections. When the ratio $\tau$ is large ($\tau=1\,000$), yielding occurs only in the cross sections of the longest post. When the ratio $\tau$ becomes small, yielding appears in the cross sections of the short post. Fig. 9 shows the relationship between the ultimate strength defined by the amplitude of the sinusoidal acceleration and the ratio $\tau$. The total slenderness ratio $\lambda_T$ in the abscissa is defined by the following expression :

$$\lambda_T=L_S/\sqrt{(I_A+I_G)/A_A} \quad \cdots\cdots (1)$$

in which $A_A$ is the area of the arch rib, $I_A$ and $I_G$ are the cross sectional moment of inertia of an arch rib and a stiffening girder respectively. The result in the case of the two-hinged arch rib is also added in this figure. When the arch bridges with the stiffening girder collapse within ten cycles of application of the sinusoidal acceleration, the acceleration amplitude decreases significantly with the increase of the total slenderness ratio. However, the dynamic strength of the arch bridge with the stiffening girder whose $\tau$ is equal to 1 000 is almost the same as that of the two-hinged arch.

### (2) Influence of longitudinal supporting condition of stiffening girder

The stiffening girder has the following three supporting conditions : a) roller-roller (type A), b) roller-hinged (type B) and c) hinged-hinged (type C). The static ultimate strength of type A is smaller and the first natural period is much longer than that of other two types. The arch rib's slenderness ratio $\lambda_A$ is taken as 300. There is no difference between type B and type C in the static ultimate strength and the first natural period. However, there are significant differences in the failure configurations in the static analysis and first vibrational mode shapes. The arch bridge of type A collapses within ten cycles of

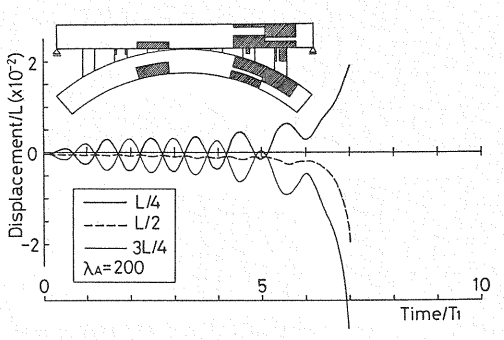


Fig. 8 Vertical displacement response of stiffened arch rib under sinusoidal acceleration.

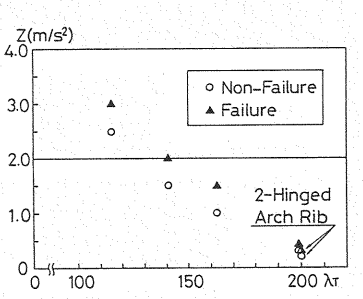


Fig. 9 Relationship between total slenderness ratio and dynamic strength.

application of the sinusoidal acceleration, whose amplitude is relatively small ($Z=1.0$ m/s$^2$), though the other two types of arch bridges do not collapse even for $Z=10$ m/s$^2$. Fig. 10 shows the yielded zones of cross sections just before the ultimate state for type A and at a certain time point during the tenth cycle for type B. For type A, two plastic hinges are formed in the arch rib at the ultimate state and yielded zones are spreading in the stiffening girder's and the posts' cross sections. For type B, the horizontal thrust of the hinged support becomes larger than that of the arch rib and produces alternatively the full tensile and compressive yielding in the stiffening girder's cross sections in the vicinity of the hinged support. For type C, the horizontal reaction at the hinged supports does not become large and yielding does not occur in any cross section. This type of support condition gives the stiffened deck arch bridges the highest dynamic strength. But the arch bridge of type C may be not adopted in practical design because thermal stresses are expected to be significant.

### (3) Influence of detailing of arch crown

The actual stiffened arch bridge usually has the central post at the crown between the arch rib and the stiffening girder. When the length of the central post is relatively short, the first vibrational mode shape, the static failure configuration and the dynamic strength of the arch bridge with the stiffening deck are almost the same as those of the arch bridge whose arch rib is rigidly connected to the stiffening girder. Fig. 11 (a) shows the yielded zones in the cross sections at the ultimate state for the stiffened arch bridge with the central post, whose length is 2 m, subjected to the sinusoidal acceleration ($Z=1.0$ m/s$^2$). The yielded zones spreads into the arch structure also in the similar manner to that of the rigidly connected stiffened arch bridge shown in Fig. 10 (a). No significant differences in the resultant horizontal shearing force and the bending moment of the each post are noted in the both types of the arch bridges with the stiffening girder.

By the conventional design method, the cross section of the central post is designed to resist against the longitudinal inertia force which is given by the product of the total weight of the stiffening girder and the seismic coefficient. The longitudinal inertia force of this arch bridge with the stiffening girder is calculated to be about 312 kN where the seismic coefficient is taken as 0.2. But in this ultimate strength analysis, the resultant shearing force is about 196 kN and the bending moment is about 294 kNm in the central post and other posts. The longitudinal inertia force of the stiffening girder is not carried by the only central post, but by all posts uniformly in spite of the difference of the rigidity of the posts.

However, when the length of the central post becomes longer, the arch rib vibrates longitudinally to the opposite direction against the stiffening girder and the deformations of all the posts become significantly larger. Consequently, the vibrational energy is absorbed by the yielding of the cross sections of the posts. For example, the stiffened arch structures with the central post whose length is 10 m does not collapse within ten cycles of application of the sinusoidal acceleration for $Z=5.0$ m/s$^2$.

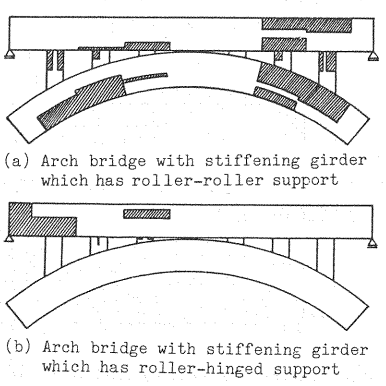

(a) Arch bridge with stiffening girder which has roller-roller support

(b) Arch bridge with stiffening girder which has roller-hinged support

Fig. 10 Yielded zones of rigidly connected stiffened arch.

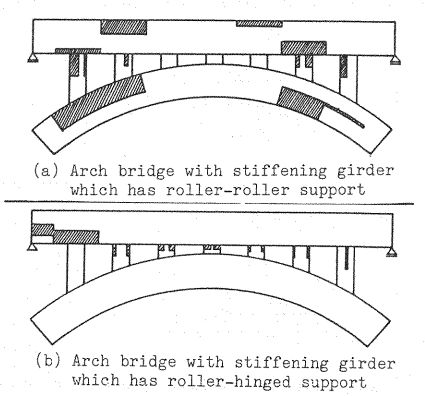

(a) Arch bridge with stiffening girder which has roller-roller support

(b) Arch bridge with stiffening girder which has roller-hinged support

Fig. 11 Yielded zones of stiffened arch with central post.

When the stiffening girder of the stiffened deck arch bridge with a central post has the roller-hinged support, the arch bridge does not collapse within ten cycles of application of the sinusoidal acceleration for $Z=10.0\ \mathrm{m/s^2}$. The yielding by bending spreads extensively into the posts' cross sections, especially into the central post's cross section in Fig. 11 (b) in comparison with the yielded zones of the rigidly connected stiffened deck arch bridge shown in Fig. 10 (b). This implies that all posts of the stiffened deck arch bridge with a central post resist against the longitudinal inertia forces of the arch rib. On the other hand, a large part of the inertia forces is taken by the connection rigidly connecting the arch rib and the stiffening girder at the crown. The cross sectional force of the central post becomes larger than those of other posts, because this vibrational mode shape is different from that of the arch bridge with the stiffening girder which has the roller-roller support. When the stiffening girder has the roller-hinged support, the dynamic strength of the stiffened deck arch bridge with a central post becomes larger than that of the arch bridge with the stiffening girder which has the roller-roller support. But the horizontal thrust produced in the hinged support of the stiffening girder becomes larger than that of the arch rib and the stiffening girder will suffer almost the yield axial force in the vicinity of the hinged support.

## 5. DYNAMIC CHARACTERISTICS OF ARCH BRIDGE STRUCTURES

The whole results analyzed here are summarized in Table 1. The slenderness ratio of the arch rib, the flexural rigidity ratio of the arch rib to the stiffening girder, the longitudinal support condition of the stiffening girder, the static ultimate strength and the first natural period are shown in this table. The static ultimate strength is given by the ratio to the full plastic load which produces the squash axial force at the springing evaluated by the first order elastic analysis[2]. Furthermore, $Z_1$ is the amplitude of the sinusoidal acceleration when the arch structures collapse within ten cycles of application of the sinusoidal acceleration and $Z_2$ is the one when the arch bridges do not collapse in Table 1. Even the application of the small amplitude of the sinusoidal acceleration leads the arch bridge to failure, when the first natural period is long. While the strong acceleration does not always lead the arch bridge to failure, when the first natural period is short. Therefore, it will become convenient for bridge designers, if they can predict the approximate ultimate strength of arch bridges which has the different arch spans, gravity mass loads and so on. Then, in order to get the nondimensional amplitude of the sinusoidal acceleration independent of the first natural period, the yield strength ratio, which is defined as the ratio of an acceleration which produces yielding to a peak acceleration, may be introduced here as follows:

$$\gamma=Q_y/(MZ_{\max}) \quad (2)$$

in which $M$ is the mass of the system and $Q_y$ is the yield restoring force which is considered to be expressed by the product of the stiffness $K$ of the system and the yield displacement $\delta_y$. Considering that the difficulty of exact specifying of $K$, $M$ and $\delta_y$, the following approximated expression may be introduced:

$$\gamma=(2\pi/T_1)^2\delta_y/Z_{\max} \quad (3)$$

Table 1 Summary of dynamic characteristics of arch structures.

| $\lambda_A$ | $\tau$ | support condition | $L_{cp}$ | $P_{cr}$ | $P/P_{cr}$ | $T_1$ | $Z_1$ | $Z_2$ | $\gamma_1$ | $\gamma_2$ |
|---|---|---|---|---|---|---|---|---|---|---|
| 150 | ∞ | - | - | 0.952 | 0.5 | 2.405 | 0.4 | 0.3 | 2.63 | 3.51 |
| 200 | ∞ | - | - | 0.795 | 0.5 | 3.298 | 0.3 | 0.2 | 2.46 | 3.69 |
| 200 | 1000 | R-R | - | 0.850 | 0.5 | 3.334 | 0.5 | 0.3 | 1.35 | 2.24 |
| 200 | 2.0 | R-R | - | 0.981 | 0.5 | 2.199 | 1.5 | 1.0 | 0.78 | 1.17 |
| 200 | 1.0 | R-R | - | 1.0 | 0.5 | 1.866 | 2.0 | 1.5 | 0.84 | 1.12 |
| 200 | 1.0 | R-R | - | 1.0 | 0.8 | 2.814 | 1.0 | 0.5 | 0.74 | 1.48 |
| 200 | 0.5 | R-R | - | 1.012 | 0.5 | 1.543 | 3.0 | 2.5 | 0.80 | 0.96 |
| 300 | ∞ | - | - | 0.395 | 0.5 | 3.803 | 0.3 | 0.2 | 4.40 | 6.60 |
| 300 | 1.0 | R-R | - | 0.869 | 0.5 | 3.135 | 1.0 | 0.5 | 0.86 | 1.71 |
| 300 | 1.0 | R-H | - | 0.956 | 0.5 | 1.231 | - | 10.0 | - | 0.34 |
| 300 | 1.0 | H-H | - | 0.95 | 0.5 | 1.204 | - | 10.0 | - | 0.35 |
| 300 | 1.0 | R-R | 2.0 | 0.878 | 0.5 | 2.836 | 1.0 | 0.5 | 1.05 | 2.11 |
| 300 | 1.0 | R-H | 2.0 | 0.952 | 0.5 | 1.334 | - | 10.0 | - | 0.28 |
| 300 | 1.0 | R-R | 10.0 | 0.825 | 0.5 | 2.850 | - | 5.0 | - | 0.20 |

R-R : roller-roller support R-H : roller-hinged support
H-H : hinged-hinged support $L_{cp}$ : length of central post
$P_{cr}$ : static ultimate strength $T_1$ : 1st natural period

where $(K/M)$ is taken equal to $(2\pi/T_1)^2$ and $\delta_y$ equal to the maximum vertical displacement of the arch rib, when a initial yielding occurs in the arch rib's cross section in the static ultimate analysis. Then, $\gamma_1$ and $\gamma_2$ in Table 1 are obtained by substituting $Z_1$ and $Z_2$ into Eq. (3). The yield strength ratio of the critical accelerations, which lead the stiffened deck arch bridges to failure or not, is almost constant regardless of the first natural period, when the stiffening girder has the roller-roller support. But, this yield strength ratio does not agree with the critical yield strength ratio corresponding to those of the two-hinged arch ribs and the arch bridges with the stiffening girder which has the roller-hinged or hinged-hinged support. This may come from the differences in vibrational modes and the exact $K$, $M$ and $\delta_y$ of the system being not employed.

## 6. CONCLUSIONS

In this paper, the in-plane dynamic strength characteristics of two-hinged steel arch ribs and arch bridges with the stiffening deck subjected to the longitudinal periodic and seismic motion of support is investigated numerically. The effect of the axial force on the ultimate strength of arch structures is examined by applying the various gravity mass load. In the analyses, the yielding of the material is taken into account in the finite deformations, but the residual stresses, the viscous and structural damping are not considered.

Some important findings are obtained through this study as follows :

(1) Two-hinged arch ribs excited by the longitudinal sinusoidal acceleration whose period is equal to their first natural period always collapse developing the antisymmetrical vibration . The process up to collapse is not affected by the slenderness ratio in the practical region, but the dynamic strength becomes smaller slightly as the slenderness ratio becomes larger.

(2) Two-hinged arch ribs subjected to the actual earthquake such as the 1940 El-Centro N-S component shows the same process up to collapse as those subjected to the sinusoidal acceleration . The static ultimate strength of the two-hinged arch rib analyzed here shows a decrease of about 10 % by the dynamic effect of the 1940 El-Centro earthquake.

(3) The arch bridges with the stiffening girder which has the roller-roller support under the longitudinal sinusoidal acceleration shows the same process up to collapse as those of the two-hinged arch ribs . The dynamic strength of arch bridges with the stiffening girder decreases significantly, as the ratio of the flexural rigidity of the arch rib to the stiffening girder becomes larger.

(4) The dynamic strength and stress distributions of stiffened deck arch bridges are affected by the longitudinal supporting condition of the stiffening girder . The dynamic strength of the stiffened deck arch bridge becomes larger, when the stiffening girder has the roller-hinged support, but it must be noted that yielding occurs in the hinged support of the stiffening girder.

(5) There are not significant differences in the dynamic strength characteristics between the stiffened deck arch bridges with the central post at the crown which has the relatively short length and arch bridges with the rigid connection between the arch rib and stiffening girder. However, the posts' cross sections of the stiffened deck arch bridges with the central post yield widely, when the stiffening girder has the roller-hinged support.

## ACKNOWLEDGEMENT

This study has been supported in part by the Grand-in-Aid for Scientific Research from the Japanese Ministry of Education, Science and Culture.

### REFERENCES

1) Kuranishi, S. and Yabuki, T. : Some numerical estimation of ultimate in-plane strength of two-hinged steel arches, Proc. of JSCE, No. 287, pp. 155~158, July, 1979.

2) Kuranishi, S., Sato, T. and Otsuki, M. : Load carrying capacity of two hinged steel arch bridges with stiffening deck, Proc. of

JSCE, No. 300, pp. 121～130, August, 1980.

3) Kuranishi, S. and Yabuki, T. : Ultimate strength design criteria for two-hinged steel arch structures, Proc. of JSCE, Structural Eng. /Earthquake Eng. Vol. 1, No. 2, pp. 229～237, October, 1984.

4) Shinke, T., Zui, H. and Nakagawa, T. : In-plane load carrying capacity of 2-hinged arches with a stiffening girder, Proc. of JSCE, No. 301, pp. 47～59, September, 1980 (in Japanese).

5) Aida, T., Saeki, H. and Kubota, A. : Analysis of elastic stability of framed structures subjected to the periodic loads, Proc. of JSCE, No. 249, pp. 29～39, May, 1976 (in Japanese)

6) Gregory, W. E. and Plaut, R. H. : Dynamic stability boundaries for shallow arches, Proc. of ASCE, Vol. 108, No. EM 6, pp. 1036～1050, December, 1982.

7) Kuranishi, S. and Nakajima, A. : Dynamic strength characteristics of axially loaded columns subjected to periodic lateral acceleration, Proc. of JSCE, No. 341, pp. 41～49, January, 1984.

(Received Novembor 13 1985)